International Journal of Minerals, Metallurgy and Materials
Volume 26, Number 11, November 2019, Page 1364
https://doi.org/10.1007/s12613-019-1857-y

Kinetics and mechanism of natural wolframite interactions with sodium carbonate

Evgeniy Nikolaevich Selivanov, Kirill Vladimirovich Pikulin, Lyudmila Ivanovna Galkova, Roza Iosifovna Gulyaeva, and Sofia Aleksandrovna Petrova

Institute of Metallurgy of the Ural Branch of the Russian Academy of Sciences, Ekaterinburg 620016, Russia
(Received: 26 December 2018; revised: 23 May 2019; accepted: 3 June 2019)

Abstract: The kinetics and mechanism of natural wolframite interactions with sodium carbonate during air heating were studied. X-ray phase and X-ray microanalysis were used to establish that the initial monocrystalline wolframite consists of $Fe_{0.5}Mn_{0.5}WO_4$ and $Fe_{0.3}Mn_{0.7}WO_4$. Differential thermal analysis showed that the interaction of wolframite with sodium carbonate begins above 450°C with the formation of tungstate, sodium ferrite, iron oxides, and manganese. Model experiments on sintering with the subsequent removal of water-soluble compounds (leaching) tracked the change in the structure of wolframite. The atomic ratio of Fe/Mn in wolframite does not change up to 600°C, and subsequently decreases to 0.2 during heating, which allows the mechanism of the process to be identified and indicates the greater reactivity of wolframites with an increased proportion of iron. Thermal analysis with data processing using non-isothermal kinetics established that the interaction of wolframite with sodium carbonate in an air stream proceeds via a two-stage mechanism, wherein the first stage is limited by diffusion (activation energy, E = 243 kJ/mol) and the second stage is limited by autocatalysis (activation energy, E = 212 kJ/mol) due to the formation of a Na_2WO_4–Na_2CO_3 eutectic.

Keywords: wolframite; structure; sodium carbonate; sintering; thermal analysis; kinetics

1. Introduction

In the industrial practice of wolframite concentrate processing, the most widespread technology includes sintering with soda, water leaching of sodium compounds, and precipitation of $CaWO_4$ [1] as a half product for the synthesis of pure oxide and metal. An important element of the technology is sintering of tungsten with calcined soda [1–4] to convert tungsten from $Fe_xMn_{1-x}WO_4$ to water-soluble Na_2WO_4.

A large amount of information exists on the process of tungsten-containing raw materials by sintering with alkali metal carbonates [5–9], however publications on the kinetics and chemistry of the interaction in $Fe_xMn_{1-x}WO_4$–Na_2CO_3 mixtures during heating are very limited. Researchers [10–11] concluded that there is a two-stage mechanism for the interaction of wolframite with sodium carbonate during heating of their mixtures. Initially, solid-phase reactions occur with the formation of Na_2WO_4. This stage is characterized by a kinetic regime with activation energy of 407 kJ/mol. Above 975°C, the interaction is limited by the diffusion of the reactants and the activation energy decreases to 18.8 kJ/mol, confirmed by the appearance of the eutectic of the Na_2WO_4–Na_2CO_3 system.

According to other research [12], the sintering of a low-grade hubnerite concentrate with sodium sulfate at 700–900°C occurs in one stage and is characterized by an activation energy of approximately 313 kJ/mol. The limiting stage of the process determines the diffusion of sodium sulfate through the layer of reaction products to the reaction surface and the discharge of interaction products.

According to [13–14], the interaction of tungstates for polyvalent d-block elements (Mn, Fe, Co) with sodium carbonate is characterized by three stages. The first stage is the ion exchange of reagents with the formation of sodium tungstate and unstable manganese carbonates (Fe, Co), the

Corresponding author: Kirill Vladimirovich Pikulin E-mail: pikulin.imet@gmail.com

second is the dissociation of carbonates with the formation of oxides(II) that are unstable at elevated temperatures, and the third is oxidative–reduction reactions converting metal oxides to higher valence state.

The interaction of WO_3 with Na_2CO_3 is thermodynamically possible [14], but the rate of reaction [15] is low due to kinetic difficulties and high-energy values of crystal lattices, 2.3 and 24.2 MJ/mol for Na_2CO_3 and WO_3, respectively. The activation energy of the WO_3 reaction with Na_2CO_3 varies [16] from 347.8 to 372.9 kJ/mol depending on the calculation method. Intensification of the solid-phase interaction of reagents is possible by introducing sulfate or sodium nitrate into the reaction mixture, as well as replacing Na_2CO_3 with $Na_2C_2O_4$ [15].

The interaction of the sintering process of a tungsten-containing concentrate with sodium carbonate was described by a one-step model for autocatalytic reactions [17]. An assumption was made regarding a change in the atomic ratio Fe/Mn in the wolframite during its sintering with soda. Notably, in addition to $Fe_xMn_{1-x}WO_4$, the studies were conducted with a concentrate containing related compounds, such as Al_2SiO_5, FeS_2, FeAsS, and SiO_2.

Despite previous studies, the mechanism and kinetic parameters of the wolframite interaction with sodium carbonate require clarification. It is assumed that the kinetics of the process is influenced not only by accompanying impurities but also by the structure of wolframite. The purpose of this work is to study the kinetics and mechanism of the interaction of natural wolframite with sodium carbonate during sintering.

2. Experimental

A natural monocrystal of wolframite (Akchatau, Kazakhstan)-(Fe, Mn)WO_4, containing 61.1wt% W, 6.1wt% Fe, 10.9wt% Mn, 0.34wt% Si, was used as the initial sample. The original crystal had dimensions of ~4 cm × 4 cm × 2 cm, and was crushed to a fraction of 0.1 mm before the experiments. Sodium carbonate of "analytical reagent" qualification contained at least 99.2wt% Na_2CO_3.

Electron probe microanalysis (EPMA) was performed using a TESCAN MIRA 3 LMU scanning electron microscope and an Oxford INCA Energy 350 X-max 80 energy dispersive X-ray spectrometer. X-ray phase analysis (XRPA) and X-ray diffraction (XRD) analysis of the formed products were performed on a Shimadzu XRD-7000 diffractometer (Cu-K_α-radiation, graphite monochromator, Bragg-Brentano focusing) with angle range 15.0°–80.0°, a shooting increment of 0.02° by 2θ, and exposure of 2 s. The ICDD PDF-2 database [18] was used to decipher the XRD patterns. A Brucker D8 Advance diffractometer (Cu-K_α-radiation, VÅNTEC-1 position-sensitive detector, β-filter) was used to determine the unit cell parameters of wolframite. The angle interval was 5°–105° with a step of 0.021° at 2θ and an exposure time of 1500 s. Decryption was performed via the DIFFRAC plus: EVA software package and ICDD PDF-2 database. The quantitative phase composition was established by a full-profile analysis in the TOPAS program.

Thermal analysis of crushed materials (particle size less than 0.1 mm, 27.5 mg) was performed on a Netzsch STA 449 C Jupiter equipment with continuous heating of samples placed in an alundum crucible. The measurements were performed by differential scanning calorimetry (DSC) and differential thermal analysis (DTA). The samples were heated to 850–900°C at 2.5, 5, 10, and 20°C/min in streams of air or argon (30–50 ml/min). The Netzsch Thermokinetics 3.0 software package was used to calculate the kinetic parameters and estimate the reaction model [19].

Model experiments were performed with a mixture of crushed mineral (1 g) and a stoichiometric amount of sodium carbonate (0.35 g) in an alundum crucible, placed in a muffle furnace and heated at a rate of 10°C/min to the required temperature (450–800°C). After the heat treatment, the crucible was removed and cooled in air. Formed products (sintered mass) were subject to water leaching in distilled water (95°C, liquid-to-solid ratio = 15, leaching time, τ = 0.5 h) and the pulp was filtered. The phase composition of the cakes was determined by powder XRD. The chemical composition of the initial materials and interaction products was determined by atomic emission spectroscopy using a Spectroflame Modula S spectrometer.

3. Results and discussion

Diffraction lines corresponding to two solid solutions of wolframite of the $Fe_xMn_{1-x}WO_4$ type were detected on a diffractogram of the initial mineral according to XRD data (Fig. 1). Wolframite has a monoclinic syngony, a prismatic (L_2PC) symmetry class, and space group of P_2/c (C_{2h}^4) [20]. The unit cell parameters of wolframite depend on the Fe/Mn molar ratio in the mineral and increase linearly with the increase in the manganese fraction. Thus, the parameter a varies linearly [21] within 0.4729–0.4832 nm, b = 0.5702–0.5759 nm, c = 0.4966–0.5000 nm, and β = 90.00°–91.17° when the composition changes from $FeWO_4$ to $MnWO_4$.

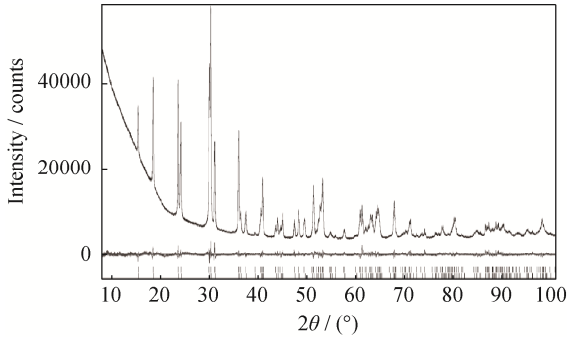

Fig. 1. X-ray powder diffraction pattern of wolframite monocrystal containing the final Rietveld refinement plot. Observed profile (top line) and its difference plot (bottom line) for $Fe_xMn_{1-x}WO_4$ in the monoclinic P_2/c space group. The vertical markers correspond to the allowed Bragg reflections: top markers—$Fe_{0.3}Mn_{0.7}WO_4$, bottom markers—$Fe_{0.5}Mn_{0.5}WO_4$.

Using the full-profile analysis according to the Rietveld method, which allows for the identification of dual (or split) X-ray reflexes, the unit cell parameters of the tungstates were determined. For the first phase, the parameters were defined as a = 0.4781 nm, b = 0.5733 nm, c = 0.4982 nm, β = 90.58° and for the second phase, were a = 0.4801 nm, b = 0.5743 nm, c = 0.4988 nm, β = 90.88°. The composition of wolframites, determined from the parameters of the unit cell [21], considering the measurement error, corresponds to the formulas $Fe_{0.5}Mn_{0.5}WO_4$ and $Fe_{0.3}Mn_{0.7}WO_4$.

The composition of the mineral was specified by X-ray microanalysis. According to the local probing data of the phases (Fig. 2), the composition of wolframite varies within the following ranges: 59.0wt%–62.6wt% W, 9.5wt%–14.7wt% Mn, 4.7wt%–8.8wt% Fe (Table 1). Adjusting the data to the generally accepted formula $Fe_xMn_{1-x}WO_4$ suggests that there are two compositions in the mineral wolframite: $Fe_{0.5}Mn_{0.5}WO_4$ and $Fe_{0.3}Mn_{0.7}WO_4$, which are close to those determined by XRD data. In addition, the initial sample is characterized by a large number of cracks oriented parallel to the surface of the crystal. The composition of the mineral in the areas of the cracked structure is characterized by a high content of manganese. The thickness of the layer with a reduced Fe/Mn atomic ratio around the cracks reached 100 μm.

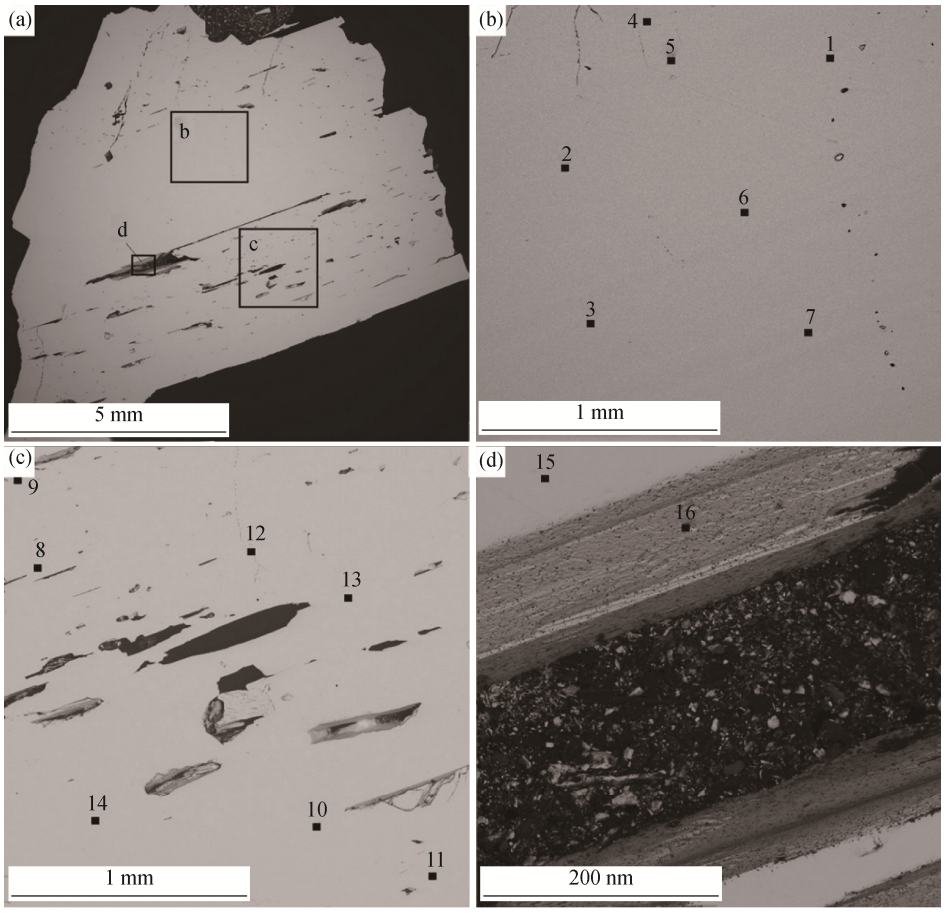

Fig. 2. Microstructure of wolframite and areas of local probing of phases: (a) general form; (b) selected b-region in (a); (c) selected c-region in (a); (d) selected d-region in (a).

Table 1. Composition of wolframite at local probing points (according to Fig. 2)

Point number	Composition / wt%			Fe/Mn (atomic ratio)	Formulae
	Mn	Fe	W		
1	10.0	8.1	60.8	0.8	$Fe_{0.44}Mn_{0.55}WO_4$
2	9.8	8.5	60.6	0.9	$Fe_{0.46}Mn_{0.54}WO_4$
3	9.7	8.6	60.5	0.9	$Fe_{0.47}Mn_{0.54}WO_4$
4	10.3	8.2	60.4	0.8	$Fe_{0.44}Mn_{0.57}WO_4$
5	9.8	8.7	60.4	0.9	$Fe_{0.48}Mn_{0.54}WO_4$
6	9.8	8.0	61.0	0.8	$Fe_{0.43}Mn_{0.54}WO_4$
7	9.7	8.3	60.8	0.8	$Fe_{0.45}Mn_{0.54}WO_4$
8	10.2	8.2	60.5	0.8	$Fe_{0.44}Mn_{0.56}WO_4$
9	9.5	8.8	60.6	0.9	$Fe_{0.48}Mn_{0.53}WO_4$
10	10.2	7.7	61.0	0.7	$Fe_{0.41}Mn_{0.56}WO_4$
11	9.6	8.2	61.1	0.8	$Fe_{0.44}Mn_{0.53}WO_4$
12	14.7	5.1	59.0	0.3	$Fe_{0.29}Mn_{0.83}WO_{4.1}$
13	13.5	4.7	60.7	0.3	$Fe_{0.25}Mn_{0.74}WO_4$
14	13.3	4.7	60.9	0.3	$Fe_{0.25}Mn_{0.73}WO_4$
15	9.7	8.4	60.9	0.9	$Fe_{0.45}Mn_{0.53}WO_4$
16	10.6	5.7	62.6	0.5	$Fe_{0.30}Mn_{0.57}WO_{3.9}$

As shown in the TG curve in Fig. 3(a), the change in sample mass does not exceed 0.1% in temperature range of 30 to 1000°C. DSC up to 1000°C (20°C/min) under airflow on the heat flow curve did not reveal transformations in the structure of the mineral. According to Fig. 3(b), for a mixture of wolframite with sodium carbonate during heating (DTA) in airflow up to 200°C, a 3.6% decrease in sample mass was associated with the removal of moisture from the reagent mixture, primarily hygroscopic Na_2CO_3. Above 420°C, the change in sample mass is associated with the interaction of wolframite and Na_2CO_3, accompanied by the release of CO_2 (gas), resulting in a loss of sample mass of 8.6%. The extreme values traced on the differential mass change curve (DTG) correspond to the moisture removal and chemical interaction of reagents. In sync with the DTG curve, the endothermic effects (start/extreme value) of moisture removal at 88/108°C and the melting of eutectic Na_2CO_3–Na_2WO_4-585/593°C are recorded on the DTA curve. In addition, the effect of 659/683°C was recorded, which corresponds to the melting of Na_2WO_4 [22–23]. Varying the heating rate within 2.5–20°C/min had little effect on the temperature of the endothermic effects. XRPA of the interaction products revealed sodium tungstate and oxides of iron and manganese (Table 2).

Heating of wolframite with soda in a stream of argon, presented on Fig. 3(c), is accompanied by endoeffects (DTA) at 580/602°C and 660/683°C. In comparison with the experiment in air, the onset temperature of the interaction for the reactants increases to 580°C and the magnitude of the mass change rate (DTG curve) increases as well. The maximum rate of mass change during heating in argon is much greater than in air. The total mass loss of the sample when heated in

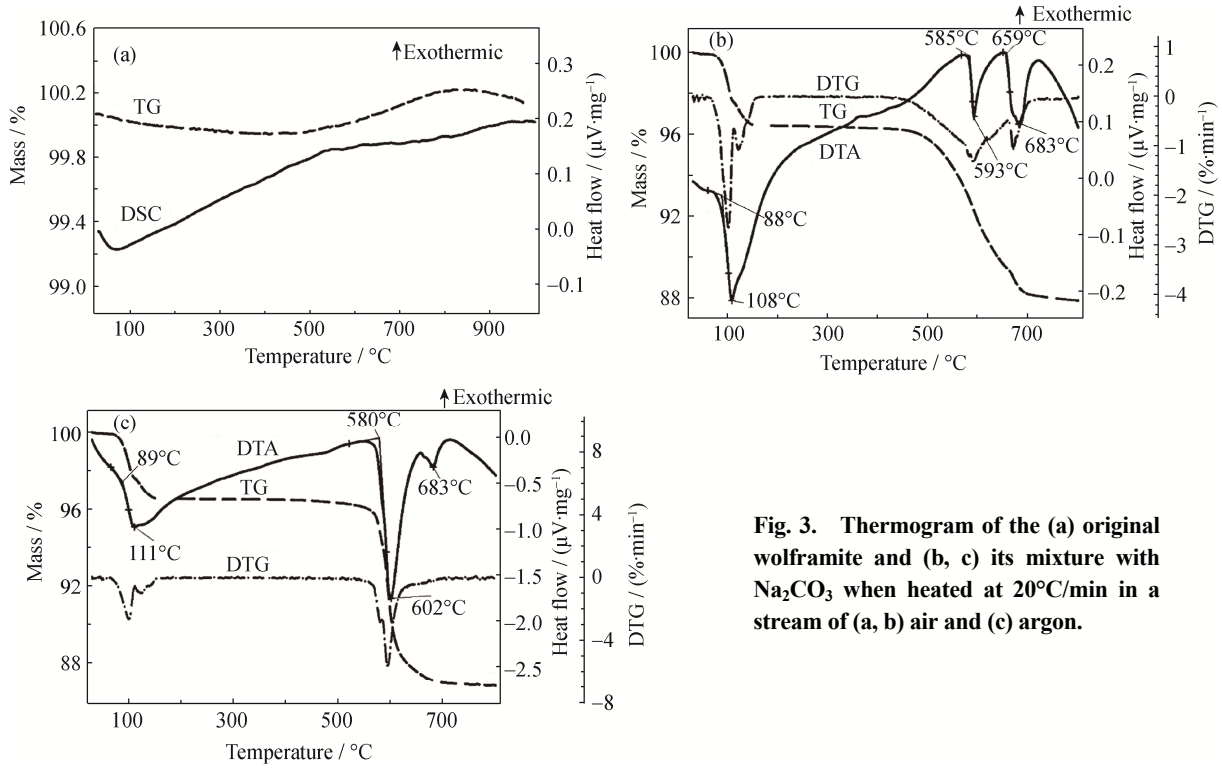

Fig. 3. Thermogram of the (a) original wolframite and (b, c) its mixture with Na_2CO_3 when heated at 20°C/min in a stream of (a, b) air and (c) argon.

Table 2. Phase composition for sintering products of wolframite mixtures with sodium carbonate under continuous heating in air

Synthesis sample No.	Final temperature / °C	Mass change / %	Phase composition of the interaction products
1	450	0.7	$Fe_{0.5}Mn_{0.5}WO_4$, $Fe_{0.3}Mn_{0.7}WO_4$, Na_2CO_3, Na_2WO_4
2	500	0.7	$Fe_{0.5}Mn_{0.5}WO_4$, $Fe_{0.3}Mn_{0.7}WO_4$, Na_2CO_3, Na_2WO_4, $NaFeO_2$
3	550	2.7	$Fe_{0.5}Mn_{0.5}WO_4$, $Fe_{0.3}Mn_{0.7}WO_4$, Na_2WO_4, Na_2CO_3, $NaFeO_2$, Fe_2O_3(traces), Mn_3O_4(traces)
4	600	6.5	$Fe_{0.5}Mn_{0.5}WO_4$, $Fe_{0.3}Mn_{0.7}WO_4$, Na_2WO_4, Na_2CO_3, $NaFeO_2$, Fe_2O_3, Mn_3O_4
5	700	9.2	Na_2WO_4, Fe_2O_3, Mn_2O_3, $Fe_{0.1}Mn_{0.9}WO_4$(traces)
6	800	9.1	Na_2WO_4, Fe_2O_3, Mn_2O_3, $Fe_{0.2}Mn_{0.8}WO_4$(traces)

argon, compared with air, is somewhat greater, which is explained by the formation of iron and manganese oxides of lower valence.

Model experiments (muffle furnace, 1 g sample, air) for specifying the composition of the phases during wolframite sintering with soda allowed for scaling the experiment and synthesis of samples suitable for leaching and estimation of the formed cakes composition. According to the XRPA of non-isothermal heating of products (Table 2), the interaction of wolframite with sodium carbonate begins at temperatures above 450°C with the formation of sodium tungstate, sodium ferrite, as well as iron and manganese oxides. A slightly smaller decrease in the mass of the sample upon heating to 800°C, in comparison with previous experience (700°C), is associated with the complete transition of iron and manganese oxides to a higher valence state. There is practically no change in the mass of the sample above 700°C, indicating the process is close to completion.

Products obtained by wolframite sintering with sodium carbonate were subjected to water leaching, after which the phase composition of the solid residues (cakes) was specified. In the course of leaching, Na_2WO_4, $NaFeO_2$, and Na_2CO_3 were transferred into the solution, which resulted in the solid residue enriched with the content of iron and manganese oxides. The main components of water leaching cakes (Table 3) are wolframite, manganese oxides-Mn_3O_4, iron(III) oxides, as well as their hydrates FeOOH and $Na_xMnO_{2.8}H_{1.6}$ (structural type $Mg_{0.25}MnO_{2.8}H_{1.6}$). In the sintered mass leaching cakes, tungsten-containing phases are represented by wolframites: $Fe_{0.5}Mn_{0.5}WO_4$ and $Fe_{0.3}Mn_{0.7}WO_4$. The composition of the cakes is influenced by the genesis of the original sample. An increase in the temperature and, therefore, the completeness of the transition of $Fe_xMn_{1-x}WO_4$ to Na_2WO_4, ensures a decrease in the tungsten-containing compounds in the leaching cakes. In the leaching cakes, the synthesis of which was performed at 700–800°C, traces of wolframite with an increased manganese content, $Fe_{0.1-0.2}Mn_{0.8-0.9}WO_4$, were observed.

Table 3. Phase composition of leaching cakes for sintering products (initial samples according to Table 2)

Sample No.	Filter cake yield / %	Phase composition (Fraction / wt%)
1	66.9	$Fe_{0.5}Mn_{0.5}WO_4$ (62.5), $Fe_{0.3}Mn_{0.7}WO_4$ (37.5)
2	68.4	$Fe_{0.5}Mn_{0.5}WO_4$ (61.7), $Fe_{0.3}Mn_{0.7}WO_4$ (38.3)
3	58.5	$Fe_{0.5}Mn_{0.5}WO_4$ (57.1), $Fe_{0.3}Mn_{0.7}WO_4$ (41.1), Fe_2O_3 (0.9), Mn_3O_4 (0.8)
4	47.7	$Fe_{0.5}Mn_{0.5}WO_4$ (46.5), $Fe_{0.3}Mn_{0.7}WO_4$ (41.1), $Me_xMnO_{2.8}H_{1.6}$ (6.7), Fe_2O_3 (3.4), Mn_3O_4 (2.1)
5	21.3	Mn_2O_3 (68.7), Fe_2O_3 (21.3), $Na_xMnO_{2.8}H_{1.6}$ (3.5), FeOOH (2.4), $Fe_{0.1}Mn_{0.9}WO_4$ (2.3), Mn_3O_4 (1.8)
6	21.5	Mn_2O_3 (71.9), Fe_2O_3 (14.0), $Na_xMnO_{2.8}H_{1.6}$ (8.0), FeOOH (3.1), $Fe_{0.2}Mn_{0.8}WO_4$ (1.8), Mn_3O_4 (1.1)

The unit cells parameters (Table 4) of wolframites remaining in the leaching cake and their composition did not change in Samples 1–4. However, in samples whose preparation was coupled with heating up to 700–800°C, the atomic ratio of Fe/Mn in wolframite was 0.2. The preferred interaction with soda for wolframite with a high iron content can then be studied, and the initial stage of the sintering process is represented in Eq. (1).

$$Fe_xMn_{1-x}WO_4 + 1.5yNa_2CO_3 + 0.25yO_2 = Fe_{x-y}Mn_{1-x}W_{1-y}O_{4-4y} + yNa_2WO_4 + yNaFeO_2 + 1.5yCO_2 \quad (1)$$

The calculations of the kinetic parameters of the interaction of wolframite with soda in air are based on thermogravimetric analysis data (Fig. 4) obtained by heating the samples at 2.5, 10, and 20°C/min. To describe the experimental data, the model-free Friedman method [24–26] was used, in which the general kinetic equation are presented as Eqs. (2) and (3).

$$d\alpha/dt = f(\alpha)k(T) \quad (2)$$

$$k(T) = A\exp\left(-\frac{E}{RT}\right) \quad (3)$$

where α is the degree of transformation adopted as the ratio of the fixed and maximum mass changes, t is the duration of the experiment, T is the temperature, $f(\alpha)$ is the function defining the reaction model, $k(T)$ is the rate constant, A is the pre-exponential multiplier, E is the activation energy, and R is universal gas constant.

Table 4. Unit cells parameters and composition of wolframites remaining in the leaching cakes

Sample No.	Wolframite primitive cells parameters				Composition of wolframites	Fe/Mn (molar ratio)
	a / nm	b / nm	c / nm	β / (°)		
Initial	0.4781	0.5733	0.4982	90.58	$Fe_{0.5}Mn_{0.5}WO_4$	1.00
	0.4801	0.5743	0.4988	90.88	$Fe_{0.3}Mn_{0.7}WO_4$	0.43
1	0.4781	0.5732	0.4982	90.60	$Fe_{0.5}Mn_{0.5}WO_4$	1.00
	0.4802	0.5741	0.4988	90.88	$Fe_{0.3}Mn_{0.7}WO_4$	0.43
2	0.4781	0.5732	0.4982	90.59	$Fe_{0.5}Mn_{0.5}WO_4$	1.00
	0.4803	0.5740	0.4988	90.90	$Fe_{0.3}Mn_{0.7}WO_4$	0.43
3	0.4781	0.5731	0.4982	90.58	$Fe_{0.5}Mn_{0.5}WO_4$	1.00
	0.4801	0.5740	0.4987	90.92	$Fe_{0.3}Mn_{0.7}WO_4$	0.43
4	0.4781	0.5731	0.4982	90.62	$Fe_{0.5}Mn_{0.5}WO_4$	1.00
	0.4801	0.5740	0.4988	90.90	$Fe_{0.3}Mn_{0.7}WO_4$	0.43
5	0.4817	0.5746	0.4995	90.97	$Fe_{0.1}Mn_{0.9}WO_4$	0.11
6	0.4813	0.5742	0.4996	90.97	$Fe_{0.2}Mn_{0.8}WO_4$	0.22

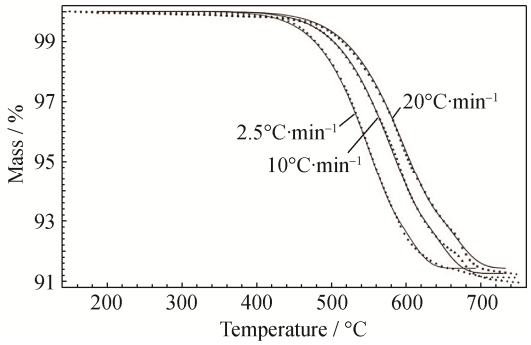

Fig. 4. Mass change of a wolframite mixture with Na_2CO_3 in air during heating at 2.5, 10, and 20°C/min. Points—experimental data; lines—model describing the reaction of the *n*th order with autocatalysis on the C component.

Application of the differential isoconversion Friedman method allows estimation of the changes for E from α [24–26]. The values of E are determined from the slope of the lines in the coordinates $\lg(d\alpha/dt)$ from $1/T$, for fixed α values (Fig. 5). The slope of the experimental curve at the beginning of the reaction is less than the slope of the isoconversion lines, indicating that the initial reaction of one-, two- or three-dimensional diffusions [19]. A no-model estimation of kinetic parameters is useful for preliminary analysis of the number of stages for the process and the probable values of E and $\lg A$. According to the obtained data, the sintering process of wolframite with sodium carbonate consists of at least two stages, the first of which is the value of E is in the range of 240–260 kJ/mol, and $\lg A$ is 12.0–14.4 (Table 5). When the degree of conversion is more than 0.7 (second stage), E decreases to 160–220 kJ/mol and $\lg A$ to 7.1–10.6.

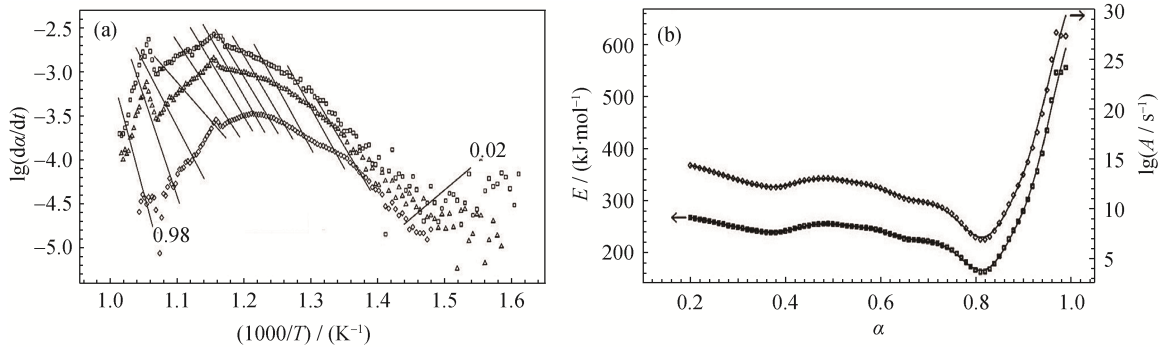

Fig. 5. Experimental data processing the interaction of wolframite with sodium carbonate (air) according to the Friedman method: (a) mass loss rate curves; (b) dependence of the activation energy and the pre-exponential factor on the mass loss of the sample.

The subsequent evaluation of the kinetic parameters of the wolframite interaction with sodium carbonate was performed by data processing using non-linear regression with two-stage process models. The experimental data are described in two consecutive stages, the first of which occurs in the diffusion (D3 or D4) mode, and the second corresponds to the reaction of the *n*th order with autocatalysis on the C component (CnC) or the *n*th order reaction (Fn). In this case, the kinetic equations of the first (D3) and second (CnC) stages during wolframite sintering with sodium carbonate can be represented by Eqs. (4) and (5) (R^2 more than 0.9995).

$$\frac{d\alpha_1}{dt} = 10^{11.9}\exp\left(-\frac{243000}{RT}\right)1.5(1-\alpha)^{\frac{1}{3}}\left[(1-\alpha)^{-\frac{1}{3}}-1\right] \quad (4)$$

$$\frac{d\alpha_2}{dt} = 10^{9.8}\exp\left(-\frac{212000}{RT}\right)(1-\alpha)^{0.99}(1+10^{-3.26}\alpha) \quad (5)$$

The established kinetic parameters (Table 6) indicate a discrepancy between the values of the activation energy and processes staging with the literatures [10–15,27] due to the variety of factors affecting the kinetics of the process, primarily differences in the composition and structure of the initial samples, the presence of impurities, and the partial pressure of oxygen.

Table 5. Changes in *E* and lg*A* from the degree of conversion (*α*) during the interaction of wolframite with sodium carbonate (Friedman method)

α / %	E / (kJ·mol^{-1})	lg(A / s^{-1})
5	245 ± 10	13.5
10	262 ± 10	14.5
20	267 ± 3	14.3
30	248 ± 3	12.9
40	241 ± 17	12.3
50	254 ± 42	13.0
60	242 ± 17	12.0
70	221 ± 4	10.6
80	166 ± 17	7.1
90	279 ± 115	13.4

Table 6. Kinetic parameters for the interaction of wolframite with sodium carbonate

Reaction type	Stage 1		Stage 2				R^2
	E_1 / (kJ·mol^{-1})	lg(A_1 / s^{-1})	E_2 / (kJ·mol^{-1})	lg(A_2 / s^{-1})	n^2	lgK_{cat}	
D3-CnC	243	11.9	212	9.8	0.99	−3.26	0.9996
D3-Fn	243	11.9	212	9.8	0.99	—	0.9996
D4-CnC	233	11.2	221	10.5	1.24	−2.59	0.9995

The mechanism of wolframite interactions with sodium carbonate can be represented as follows: at the interphase, reactions between solid reactants occur with the formation of sodium tungstate layer. The surface migration of reagents with subsequent bulk diffusion through the layer of the reaction product is likely the limiting stage of the process. A similar mechanism [28], which determines diffusion through the product layer with similar activation energy values of 297 and 184 kJ/mol, was described in the study of the interaction of WO_3 and MoO_3 with heavy metal oxides, as well as for reactions of MoO_3 with alkaline earth metal carbonates with an activation energy of 230–250 kJ/mol. At 581°C, a low-melting eutectic Na_2WO_4–Na_2CO_3 is formed in the system [22–23], diffusion difficulties decrease, and the process goes into an autocatalytic mode.

4. Conclusions

Natural monocrystal wolframite has areas that differ in the atomic ratio of Fe/Mn. In a sample of wolframite from the Akchatau deposit (Kazakhstan), the instability of the Fe/Mn ratio corresponds to the $Fe_{0.5}Mn_{0.5}WO_4$ and $Fe_{0.3}Mn_{0.7}WO_4$ compositions.

The wolframite interaction with sodium carbonate begins above 450°C with the formation of low-melting tungstate and sodium ferrite, as well as the eutectic of Na_2CO_3–Na_2WO_4. The interaction of wolframite with sodium carbonate in air proceeds via a two-stage mechanism, limited in the first stage by the diffusion of reagents to the contact surface and the removal of interaction products. The low-melting phases in the system contribute to the transition of the process to the autocatalytic mode. The activation energies of the first and second processes are 243 and 212 kJ/mol, respectively. These results are useful for the explanation of the mechanism for polycationic oxide transformation during high-temperature interactions with soda, explaining the features and substantiation of the modes of processes during the processing of wolframite concentrates.

Acknowledgements

The work was carried out according to the state assignment for IMET UB RAS and Comprehensive Program for Basic Research of the Ural Branch of the Russian Academy

of Sciences (No. AAAA-A18-118012590113-6) using equipment of Collaborative usage centre "Ural-M".

References

[1] E. Lassner and W.D. Schubert, *Tungsten: Properties, Chemistry, Technology of the Element, Alloys and Chemical Compounds*, Springer, New York, 1999.

[2] J.R.L. Trassorass, T.A. Wolfe, W. Knabl, C. Venezia, R. Lemus, E. Lassner, W.D. Schubert, E. Lüderitz, and H. Wolf, *Tungsten, Tungsten Alloys, and Tungsten Compounds*, Wiley-VCH, Weinheim, 2016.

[3] W.Z. Yang, W. Wang, X.C. Wu, K.J. Yang, Q.K. Li, and J.L. He, Co-extraction of tungsten and molybdenum from refractory scheelite–powellite blend concentrates by roasting with Na_2CO_3 and SiO_2 and leaching with water, *Can. Metall. Q.*, 57(2018), No. 4, p. 447.

[4] V.L. Dimitrijević, M.D. Dimitrijević, and D. Milanović, Recovery of tungsten from low-grade scheelite concentrate by soda ash roast-leach method, *J. Min. Metall. Sect. A*, 40(2004), No. 1, p. 75.

[5] A.A. Palant, V.A. Bryukvin, and A.V. Tovtin, Extracting tungsten from wolframite-processing waste, *Russ. Metall.*, 1999, No. 5, p. 23.

[6] B. Şirin, E. Açma, C. Arslan, and O. Addemir, The effect of sulphur on tungsten recovery from scheelite concentrates by alkali fusion, *Can. Metall. Q.*, 33(1994), No. 4, p. 313.

[7] K. Srinivas, T. Sreenivas, R. Natarajan, and N.P.H. Padmanabhan, Studies on the recovery of tungsten from a composite wolframite–scheelite concentrate, *Hydrometallurgy*, 58(2000), No. 1, p. 43.

[8] J.F. Paulino, J.C. Afonso, J.L. Mantovano, C.A. Vianna, and J.W.S.D. da Cunha, Recovery of tungsten by liquid–liquid extraction from a wolframite concentrate after fusion with sodium hydroxide, *Hydrometallurgy*, 127(2012), p. 121.

[9] K.V. Pikulin, E.N. Selivanov, L.I. Galkova, and R.I. Gulyaeva, Features of tungsten extraction from spent catalysts of petroleum organic synthesis, *Tsvetn. Met.*, 2017, No. 11, p. 31.

[10] V.L. Butuhanov and E.V. Hromtsova, *Physical–Chemical Basics of Complex Application of Mineral Tungsten Ore*, Pacific Ocean State University, Khabarovsk, 2015.

[11] G.I. Hanturgaeva, The combined technologies of complex processing of difficult-to-enrich molybdenum and tungstic ores, *Min. Inf. Anal. Bull. Sci. Technol. J.*, 14(2009), No. 12, p. 478.

[12] B.S. Ayushieva and E.V. Zoltoev, Kinetic features of the sintering process for hubnerite concentrate with sodium sulfate, *Min. Inf. Anal. Bull. Sci. Technol. J.*, 2012, No. 1, p. 125.

[13] G.K. Shurdumov, Z.A. Cherkesov, and L.I. Makaeva, Effect of mass transfer of systems $Mn(Fe,Co)Mo(W)O_4$–Na_2CO_3 and environment and need for his account when identifying molybdates and tungstates of multivalent d-elements, Mn, Fe, Co, on basis of thermogravimetric data, *Izv. Vyssh. Uchebn. Zaved. Khim. Khimich. Tekhnol.*, 62(2019), No. 2, p. 111.

[14] G.K. Shurdumov and Y.L. Kardanova, Chemical evolution $MeSO_4$–Na_2CO_3–$Mo(W)O_4$ type systems during heat treatment and the development of optimized solid phase synthesis method molybdates and tungstates d-elements family (Me-d-element), [in] *Proceeding of the Kabardino-Balkarian State University*, 6(2016), No. 2, p. 63.

[15] G.K. Shurdumov, Z.A. Cherkesov, and Z.O. Kerefov, Synthesis of sodium tungstate from the system $Na_2C_2O_4$–$NaNO_3$–WO_3, *Russ. J. Inorg. Chem.*, 52(2007), No. 5, p. 674.

[16] S.Q. Sun, Study on the chemical behavior of solid phase reaction of WO_3 and Me_2CO_3 by the method of thermal analysis, *Chem. Res. Chin. Univ.*, 6(1985), No. 2, p. 151.

[17] K.V. Pikulin, E.N. Selivanov, L.I. Galkova, and R.I. Gulyaeva, Specific features of the phase formation and process kinetic for wolframite concentrate sintering with sodium carbonate, *Khimich. Tekhnol.*, 19(2018), No. 9, p. 413.

[18] J. Faber and T. Fawcett, The powder diffraction file: present and future, *Acta Crystallogr. Sect. B: Struct. Sci*, 58(2002), No. 3, p. 325.

[19] H.J. Flammersheim and J. Opfermann, Formal kinetic evaluation of reactions with partial diffusion control, *Thermochim. Acta*, 337(1999), No. 1-2, p. 141.

[20] E. García-Matres, N. Stüßer, M. Hofman, and M. Reehuis, Magnetic phases in $Mn_{1-x}Fe_xWO_4$ studied by neutron powder diffraction, *Eur. Phys. J. B*, 32(2003), No. 1, p. 35.

[21] A. Sasaki, Variation of unit cell parameters in wolframite series, *Mineral. J.*, 2(1959), No. 6, p. 375.

[22] V.I. Posypaiko, E.A. Alexeeva, and N.A. Vasina, *Melting Diagrams of Salt Systems. P. 3*, Metallurgiya, Moscow, 1979.

[23] N.I. Kopylov, Yu.D. Kaminskii, and A.V. Polugrudov, The $NaNO_3$–Na_2CO_3–Na_2WO_4 system, *Russ. J. Inorg. Chem.*, 43(1998), No. 12, p. 1952.

[24] S. Vyazovkin, A.K. Burnham, J.M. Criado, L.A. Pérez-Maqueda, C. Popescu, and N. Sbirrazzuoli, ICTAC kinetics committee recommendations for performing kinetic computations on thermal analysis data, *Thermochim. Acta*, 520(2011), No. 1-2, p. 1.

[25] S. Vyazovkin, A unified approach to kinetic processing of non-isothermal data, *Int. J. Chem. Kinet.*, 28(1996), No. 2, p. 95.

[26] S. Vyazovkin and C.A. Wight, Model-free and model-fitting approaches to kinetic analysis of isothermal and non-isothermal data, *Thermochim. Acta*, 340-341(1999), p. 53.

[27] G.K. Shurdumov, Z.V. Shurdumova, and Z.A. Cherkesov, Synthesis of potassium tungstate in the K_2CO_3– KNO_3–WO_3, *Russ. J. Inorg. Chem.*, 54(2009), No. 1, p. 137.

[28] M.E. Brown, D. Dollimore, and A.K. Galwey, *Reactions in the Solid State*, Elsevier, Amsterdam, 1980.